Available online at www.sciencedirect.com
SCIENCE DIRECT®
International Journal of Heat and Mass Transfer 48 (2005) 1705–1715
International Journal of HEAT and MASS TRANSFER
www.elsevier.com/locate/ijhmt

Simulation of mass transfer from an oscillating microdroplet

Guoqiang Guan [a], Jiahua Zhu [a,*], Sulan Xia [a], Zhaohua Feng [a], E. James Davis [b]

[a] School of Chemical Engineering, Sichuan University, Chengdu 610065, PR China
[b] Department of Chemical Engineering, University of Washington, Seattle, Washington, DC 98195-1750, USA

Received 5 July 2004; received in revised form 24 November 2004
Available online 22 January 2005

Abstract

Mass transfer from micrometer and sub-micrometer airborne microdroplets arises in various chemical process, material science, and atmospheric phenomena, such as impinging flow reactor and unsteady pollutant diffusion, where microdroplet oscillation can substantially increase the mass transfer rate. Previous theories, however, do not adequately predict this enhancement of mass transfer, especially in the case of relatively large-amplitude oscillations. We have analyzed slow evaporation of an oscillating microdroplet having a sufficiently low vapor pressure such that it remains at the surrounding gas temperature and has a negligibly small rate of change of diameter. We solved the governing convective diffusion equation numerically to obtain the Sherwood number as a function of the system parameters. These include the oscillation frequency, the maximum velocity, and the initial microdroplet diameter. The theoretical results are compared with mass transfer data from the literature for a dodecanol microdroplet levitated in an electrodynamic balance (EDB) and oscillated by varying the dc levitation voltage and the ac amplitude and frequency. The predicted Sherwood numbers agree with the experimental results with a mean deviation of 9.2%. The analysis shows a distinct periodic change in the mass transfer rate or Sherwood number with a period that is one-half the period of oscillation of the microdroplet.

Keywords: Mass transfer; Oscillation; Electrodynamic balance

1. Introduction

There has long been an interest in the mass transfer from oscillating micrometer and sub-micrometer droplets (hereafter called microdroplets) because of their presence in various chemical processes, the atmosphere, and other processes involving nucleation, condensation, and evaporation, for example in impinging flow reactor, vibrated fluidized bed, pollutant diffusion and so on.

The oscillatory motion of a microdroplet is a classical problem in fluid mechanics considered by a number of authors. Prosperetti [1] analyzed the initial value problem of free oscillations of droplets, determining the damped oscillatory characteristics of small-amplitude free oscillations. The flow field induced by an oscillating droplet for low Reynolds numbers was described by Landau and Lifshitz [2].

Enhancement of heat and mass transfer can be accomplished by oscillating a microdroplet in the surrounding fluid. This can be achieved by mechanical, electric, or acoustic means. Chen et al. [3], for example, experimentally investigated the effects of interfacial heat

* Corresponding author. Tel.: +862 885 406869; fax: +862 885 403397.
E-mail address: jhzhu@scu.edu.cn (J. Zhu).

0017-9310/$ - see front matter © 2005 Elsevier Ltd. All rights reserved.
doi:10.1016/j.ijheatmasstransfer.2004.11.008

Nomenclature

a	microdroplet radius [m]
A	oscillatory amplitude [m]
C	mass concentration [kg/m^3]
D	diffusivity [m^2/s]
F	radial damping factor
G	tangential damping factor
i	imaginary number unit
k	complex penetration depth [m]
k_G	mass transfer coefficient [m/s]
N	mass flux [kg/(m^2 s)]
Pe	Peclet number, $2au_0/D_{ij}$
Sh	Sherwood number, $2ak_G/D_{ij}$
St	Strouhal number, $\omega a/u_0$
t	time [s]
u	microdroplet velocity [m/s]
v	fluid velocity [m/s]
W	mass transfer rate [kg/s]
z_0	position of the center of microdroplet relative to the null point [m]

Greek symbols

δ	real part of complex penetration depth [m]
v	fluid kinetic viscosity [m^2/s]
ω	angular oscillatory frequency [Hz]

Superscripts

$'$	quantities related to the r', θ' coordinate system
$*$	dimensionless quantities

Subscripts

i	mass transfer components
j	fluid media
r	radial component
s	quantities on the microdroplet surface
θ	tangential component

transfer on an oscillating water column. Oscillation was produced by means of a mechanical piston. They found that the local heat transfer coefficient near the interface increased rapidly due to the periodical renewal of the interface. Mayya [4] investigated bipolar charge-induced drift and diffusion of aerosol microdroplets in oscillating electric fields. He assumed that the microdroplets undergo diffusion charging and neglected field charging effects in his model, so his results have some similarity to diffusional mass transfer. Sujith et al. [5] described mass transfer phenomena associated with a small droplet in an acoustic field, showing a 100% increase in the mass transfer rate in the presence of a 160 dB acoustic field, and Tian and Apfel [6] studied the evaporation of arrays of droplets in an acoustic field. When the velocity of the flow field was of order 0.01 m/s, the enhancement due to convection induced by the oscillation was found to be less than 15%. Mashayek and Ashgriz [7] studied the effects of internal circulation in drops on heat transfer, motion, and deformation. Mashayek [8] examined the interaction of evaporation and deformation of drops. The rate of evaporation increased with the increase of the amplitude of the surface deformation, and the mass flux was expressed as a function of the surface curvature.

Zhu et al. [9] levitated a charged microdroplet in an electrodynamic balance (EDB). The EDB uses superposed ac and dc electric fields to trap particles, and the principles and applications of the EDB were reviewed by Davis [10]. Zhu et al. [9] varied both the dc voltage and the ac voltage and frequency to oscillate a droplet in nitrogen to achieve oscillation amplitudes as large as five times the microdroplet diameter. They found that the mass transfer rate increased by up to five times the evaporation rate for a stationary droplet in a stagnant gas.

According to Al Taweel and Landau [11], in the case of small amplitude oscillation, where the oscillation amplitude is less than 75% of the characteristic length of the droplet, the mass transfer is affected by the acoustic streaming and is well-correlated by the ratio of the oscillation amplitude and the droplet diameter (A/d). In the case of large amplitude oscillation ($A/d > 0.75$), however, the mass transfer is well predicted by a quasi-steady model. In the experiments of Zhu et al. [9], A/d varied from about 0.3 to 5.

Numerous mass transfer correlations for mass transfer with flow around spheres are found in the literature; Davis and Schweiger [12] listed many of them. For example, Zhang and Davis [13] correlated evaporation rate data for microdroplets using an interpolation formula of the form

$$Sh = 2 + [(0.5Pe + 0.3026Pe^2)^{-n} + (1.008Pe^{1/3})^{-n}]^{-1/n}. \quad (1)$$

Eq. (1) incorporates the low-Pe asymptotic solution of Kronig and Bruijsten in Ref. [9] and the high-Pe solution of Levich [14]. Zhang and Davis [13] found that for $n = 3$ Eq. (1) agrees well with experimental data for steady flow around a droplet. Zhu et al. [9] found that the mass transfer rates they measured are substantially greater than those predicted by considering Eq. (1) to valid at each point in time (a quasi-steady approximation).

Zhu et al. [9] formulated a convective diffusion equation for mass transfer using the flow field described by Landau and Lifshitz [2], but they did not solve the equation. Feng et al. [15] expanded on the theory of oscillation stability and found that there is a sub-stable condition between stable and unstable oscillation and pointed out that the mass transfer analysis needs to be updated to take large-amplitude oscillations into account.

The objective of this research was to develop a mass transfer model for an oscillating microdroplet and to compare the results with the data of Zhu et al. [9].

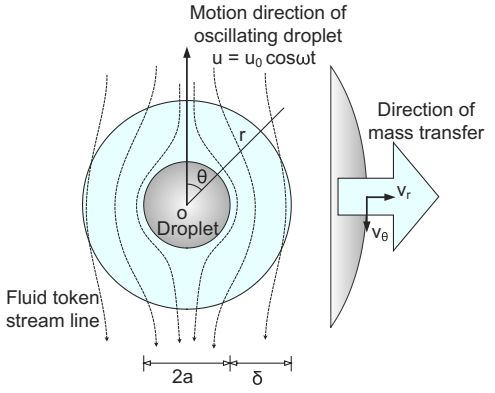

Fig. 1. Sketch of mass transfer from an oscillating microdroplet.

2. Mass transfer theory

2.1. The flow field

The low Reynolds number flow field in the vicinity of an oscillating microdroplet was derived by Landau and Lifshitz [2]. The oscillatory motion of the microdroplet is approximated by the periodic function

$$z_0 = A\sin\omega t, \tag{2}$$

where z_0 is the position of the center of the microdroplet relative to the null point of the oscillation, and ω is the frequency of oscillation.

Landau and Lifshitz [2] obtained the following fluid velocity components:

$$v_r = -2u_0 e^{-i\omega t}F(r)\sin\theta, \tag{3}$$

$$v_\theta = u_0 e^{-i\omega t}G(r)\sin\theta, \tag{4}$$

$$v_\varphi = 0, \tag{5}$$

where $F(r)$ and $G(r)$ are damping factors in the radial and tangential directions, respectively, given by

$$F(r) = \left[Ae^{ikr}\left(r - \frac{1}{ik}\right) + B\right]\frac{1}{r^3}, \tag{6}$$

$$G(r) = \left[Ae^{ikr}\left(ikr^2 - r + \frac{1}{ik}\right) - B\right]\frac{1}{r^3}, \tag{7}$$

where

$$A = -\frac{3a}{2ik}e^{ikr}, \quad B = -\frac{a^3}{2}\left(1 - \frac{3}{ika} - \frac{3}{k^2a^2}\right),$$
$$k = \frac{1+i}{\sqrt{2\nu/\omega}}. \tag{8}$$

Here, ν is the kinematic viscosity of the fluid.

2.2. Mass transfer model

We consider an isolated spherical microdroplet immersed in a gaseous medium undergoing forced oscillation while mass transfer occurs, as is illustrated in Fig. 1. Since there is axial symmetry, the problem can be considered to be a two-dimensional problem.

Let us consider the slow evaporation of a relatively low vapor pressure substance into a gas that contains no vapor at an infinite distance from the droplet surface at room temperature. Since the mass transfer is coupled to the periodic flow field, the mass transfer rate is time-dependent. If the mass transfer rate is sufficiently slow, we can neglect the size change during the time interval of interest, and the evaporation process is very nearly isothermal, as discussed by Davis and Schweiger [12] and shown by others [16,17] by analysis of the coupled heat and mass transfer processes involved with droplet evaporation and condensation. The thermal effects associated with friction are also neglected because of the low viscosity of the gas and the low Reynolds number. The electric field in the EDB is not sufficiently large to affect the mass transfer rate unless the Rayleigh limit of charge is reached, at which point a droplet explodes [18]. The microdroplet is small enough to permit us to neglect the internal circulation, and, as shown by Zhu et al. [9], no deformation of the droplet from spherical need be considered. For a dilute gas/vapor mixture, the bulk flow can be assumed to be that of the fluid surrounding the microdroplet. Assuming that the radial component of the flow dominates the mass transfer process, tangential diffusion can be neglected because the mass transfer is dominated by the quantity of material leaving the microdroplet in the radial direction. Tangential diffusion can be expected to be very small compared with tangential convection except at small Peclet numbers.

2.3. Mass transfer governing equation

To obtain the transport equation, let us introduce the coordinate system shown in Fig. 2. In the two-dimensional coordinate system let O be the origin in the inertial coordinate system (r, z), that is, O is at the center of

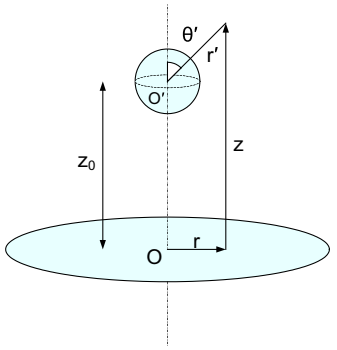

Fig. 2. Coordinate system used for the oscillating microdroplet.

the oscillation. Then let O′ be the origin of the oscillating microdroplet. A point in the fluid is identified by coordinates r' and θ' based on O′. The mass transfer equation related to the inertial coordinate system (r,z) can be expressed by the convective diffusion equation,

$$\frac{\partial C_i}{\partial t}+\mathbf{v}\cdot\nabla C_i = D_{ij}\nabla^2 C_i, \tag{9}$$

where $C_i(r,z,t)$ is the vapor concentration relative to coordinate O at time t, $\mathbf{v}$ is the fluid velocity vector, and D_{ij} is the diffusion coefficient for vapor i in carrier gas j. The concentration at the surface of the microdroplet is constant at C_{is}, and the gaseous medium contains no vapor before oscillation of the microdroplet. Thus, the initial and boundary conditions corresponding to Eq. (9) are given by

$$\begin{aligned} &C_i|_{\substack{(z,r)\in S\\ t=t}} = C_{is}, \quad S=\left\{(z,r)\middle|(z-z_0)^2+r=a^2\right\},\\ &C_i|_{\substack{(z,r)\in \overline{S}\\ t=0}} = 0, \quad \overline{S}=\left\{(z,r)\middle|(z-z_0)^2+r>a^2\right\}. \end{aligned} \tag{10}$$

It is convenient to transform Eq. (9) to the r', θ' coordinate system by means of the transformations

$$r = r'\sin\theta', \quad z = z_0 + r'\cos\theta', \tag{11}$$

where z_0 is the position of microdroplet given by Eq. (2). Eq. (9) transforms to the mass transfer governing equation in the r', θ' coordinates to give

$$\begin{aligned} &\frac{\partial C_i'}{\partial t}+\left(v_r'-\omega A\cos\omega t\cos\theta'\right)\frac{\partial C_i'}{\partial r'}\\ &\quad+\left(v_\theta'+\omega t\cos\omega t\sin\theta'\right)\frac{1}{r'}\frac{\partial C_i'}{\partial \theta'}\\ &=D_{ij}\left[\frac{2}{r'}\frac{\partial C_i'}{\partial r'}+\frac{\partial^2 C_i'}{\partial r'^2}+\frac{1}{r'^2\sin\theta'}\right.\\ &\quad\left.\times\left(\cos\theta'\frac{\partial C_i'}{\partial\theta'}+\sin\theta'\frac{\partial^2 C_i'}{\partial\theta'^2}\right)\right], \end{aligned} \tag{12}$$

where all primes signify quantities related to the r', θ' coordinate system.

Neglecting the tangential diffusion term and dropping the primes with the understanding that we are still dealing with the r', θ' coordinate system, Eq. (12) reduces to

$$\frac{\partial C_i}{\partial t}+(\mathbf{v}-\mathbf{u})\cdot\nabla C_i = D_{ij}\nabla_r^2 C_i, \tag{13}$$

where ∇_r^2 is only the radial component of the Laplacian operator.

The initial and boundary conditions become

$$C_i|_{\substack{r=a\\ t=t}} = C_{is}, \quad C_i|_{\substack{r>a\\ t=0}} = 0. \tag{14}$$

Eq. (13) is similar to the expression for the Reynolds transport theorem [19] in the case of a moving control volume. In fact, the equation can be deduced from the Reynolds transport theorem in this case.

It is convenient to write the governing equation in dimensionless form by introducing the dimensionless quantities

$$\begin{aligned} &C_i^*=\frac{C_i}{C_{is}}, \quad v_r^*=\frac{v_r}{u_0}, \quad v_\theta^*=\frac{v_\theta}{u_0}, \quad r^*=\frac{r}{a},\\ &\theta^*=\frac{\theta}{\pi}, \quad t^*=\omega t. \end{aligned} \tag{15}$$

Substituting Eq. (15) in Eqs. (8) and (9), the governing equations become

$$\begin{aligned} &St\frac{\partial C_i^*}{\partial t^*}+\left(v_r^*-\cos t^*\cos\pi\theta^*\right)\frac{\partial C_i^*}{\partial r^*}\\ &\quad+\frac{v_\theta^*+\cos t^*\sin\pi\theta^*}{r^*\pi}\frac{\partial C_i^*}{\partial\theta^*}\\ &\quad=\frac{2}{Pe}\left(\frac{\partial^2 C_i^*}{\partial r^{*2}}+\frac{2}{r^*}\frac{\partial C_i^*}{\partial r^*}\right) \end{aligned} \tag{16}$$

$$C_i^*|_{\substack{r^*=1\\ t^*=t^*}} = 1, \quad C_i^*|_{\substack{r^*>1\\ t^*=0}} = 0, \tag{17}$$

where $St=\omega a/u_0$ is the Strouhal number, and $Pe=2au_0/D_{ij}$ is the Peclet number.

2.4. The mass transfer coefficient and mass transfer rate

The mass flux at any specific tangential position is given by

$$N_i = -D_{ij}\frac{\mathrm{d}C_i}{\mathrm{d}r}+v_r C_i, \tag{18}$$

and the average mass flux over the surface of the microdroplet is

$$\overline{N}_i = \frac{1}{4\pi r^2}2\pi\int_0^\pi\left(-D_{ij}\frac{\mathrm{d}C_i}{\mathrm{d}r}+v_r C_i\right)r^2\sin\theta\,\mathrm{d}\theta. \tag{19}$$

A mass transfer coefficient, k_G, may be defined as follows [20]:

$$\overline{N}_i|_{r=a} = k_G C_{is}. \tag{20}$$

Equating Eqs. (19) and (20), and introducing the dimensionless quantities in Eq. (15), we obtain the dimensionless mass transfer coefficient or Sherwood as

$$Sh = -\int_0^1 \left.\frac{\partial C_i^*}{\partial r^*}\right|_{r^*=1} \sin\pi\theta^* \, \mathrm{d}\pi\theta^*. \quad (21)$$

Consequently, the Sherwood number can be determined from the solution of the governing equations, and the mass transfer rate is given by

$$W_i = 4\pi a^2 \overline{N}_i|_{r=a}, \quad (22)$$

where the average mass flux is given by Eq. (19).

Because the microdroplet is oscillating and the concentration profile is time-dependent, the Sherwood number and the mass transfer rate are both time-dependent. To compare the predictions with experimental results we need to integrate the mass transfer rate over an appropriate period of time.

3. The numerical solution

We used the arbitrary Lagrangian–Eulerian (ALE) method discussed by Hirt et al. [21] to discretize the computational domain. Following the framework of ALE, the mesh (101×101, structuralized equal-interval nodes) is considered to adhere to the oscillating microdroplet and move with the microdroplet. We applied a finite difference method to solve Eq. (16). The time-dependent, convective and diffusive terms in Eq. (16) were approximated by forward, second order upwind and central difference schemes, respectively. To assure numerical stability, Wei et al. [22] suggested that the time increment should satisfy the inequality, $\Delta t < \Delta x/(u + 2v/\Delta x)$. Consequently, we adopted $\Delta t = 0.5\Delta x/(u + 2v/\Delta x)$ for the time increment.

4. Mass transfer experiments

Evaporation experiments were performed by Zhu et al. [9] using an octopole EDB described by Zheng et al. [23], illustrated in Fig. 3. A dodecanol (DDA) microdroplet was electrodynamically trapped in an EDB that contained nitrogen. The alternating electric field induced the microdroplet to oscillate in a harmonic motion that is consistent with Eq. (2). A charge coupled device (CCD) linescan video camera with a 9.45× telemicroscopic lens was used to record the motion of the microdroplet, and light scattering was used to determine the radius of the microdroplet by comparing angular scattering data with Mie theory. Angular scattering data are extremely sensitive to size and shape, and small deviations from spherical can be detected. The video image also would show any distortion. The DDA microdroplet evaporation rate was determined from the light scattering data. Because of the low vapor pressure of DDA microdroplet (~0.4 Pa at 298 K) the evaporation rate was low and essentially isothermal at room temperature. Table 1 lists the data obtained by Zhu et al. [9].

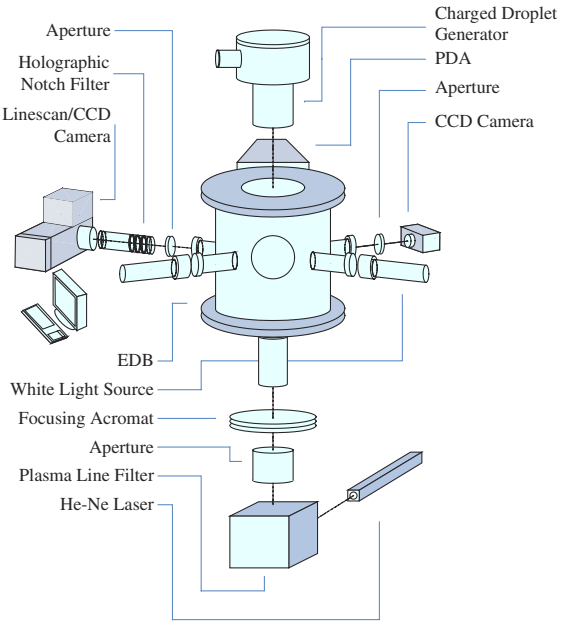

Fig. 3. Overview of the EDB system.

Table 1
A comparison of the experimental and theoretical data

Case	a (μm)	u_0 (m/s)	f (Hz)	Re	$St \times 100$	Pe	$StPe$	Sh_{expt}	Sh[a]	% Difference	Sh[b]	% Difference
1	21.05	0.187	25.0	0.635	1.718	1.440	0.025	3.733	2.972	−20.4	3.241	−13.2
2	20.15	0.343	45.9	1.148	1.694	2.603	0.044	4.175	3.355	−19.6	4.245	1.7
3	22.75	0.127	152.2	0.480	17.13	1.088	0.188	5.164	2.762	−46.5	5.759	11.5
4	23.60	0.163	198.7	0.639	18.08	1.449	0.262	10.57	2.977	−71.8	11.65	10.2
Mean deviation										39.6		9.2

[a] Based on Eq. (1) and the quasi-steady approximation.
[b] Based on the present analysis.

5. Results and discussion

5.1. Comparisons between theoretical and experimental data

The results of the mass transfer experiments by Zhu et al. [9] and the predicted Sherwood numbers based on Eq. (1) are presented in Table 1. In using Eq. (1) it is assumed that the mass transfer process is at quasi-steady state, that is, Eq. (1) is applied at each point in time using the Peclet number at that time. This quasi-steady state approach greatly underpredicts the time-averaged Sherwood number (mean deviation = 39.6%), particularly at the higher frequencies of oscillation. The calculations based on the present model are in much better agreement with the experimental results by Zhu et al. [9], the mean deviation being 9.2%. The increase in the Sherwood number as the oscillation frequency increases is more accurately predicted by the present model in this case.

For steady flow around a microdroplet the mass transfer depends on the Peclet number as shown in Eq. (1), but our analysis shows that both the Peclet number and the Strouhal number are important. Table 1 lists the *StPe* product for each of the data sets. The Sherwood number is seen to increase as the product increases, but there is not a linear relationship between *Sh* and *StPe*.

5.2. Streaming in the vicinity of the oscillating microdroplet

Streaming near the surface of oscillating microdroplet obviously inherits the periodical characteristic. Fig. 4 shows the streamlines and grayscale contours of the flow fields at particular dimensionless instants in an oscillatory cycle, i.e., 2π, 2.5π, 3π and 3.5π. Because the observation point is fixed on the center of microdroplet, referred to the reference coordinates, the flow patterns are the same as "creeping flow" patterns. When it is at 2π, the microdroplet is at the null point of the oscillation and is moving toward the right side of the figure. The flow near the surface of microdroplet is almost stagnant and the flow far from the microdroplet surface is almost at the maximum velocity. When it is at 2.5π, the microdroplet is at rest at its farthest distance from the null point. There is a slight flow toward the right side of the figure in this case. It indicates that there is a "phase drift" between the oscillation of microdroplet and fluid flow. The phenomena of "phase drift" reflects the time difference between the exciter (the oscillating microdroplet) and the responder (the flow field), which

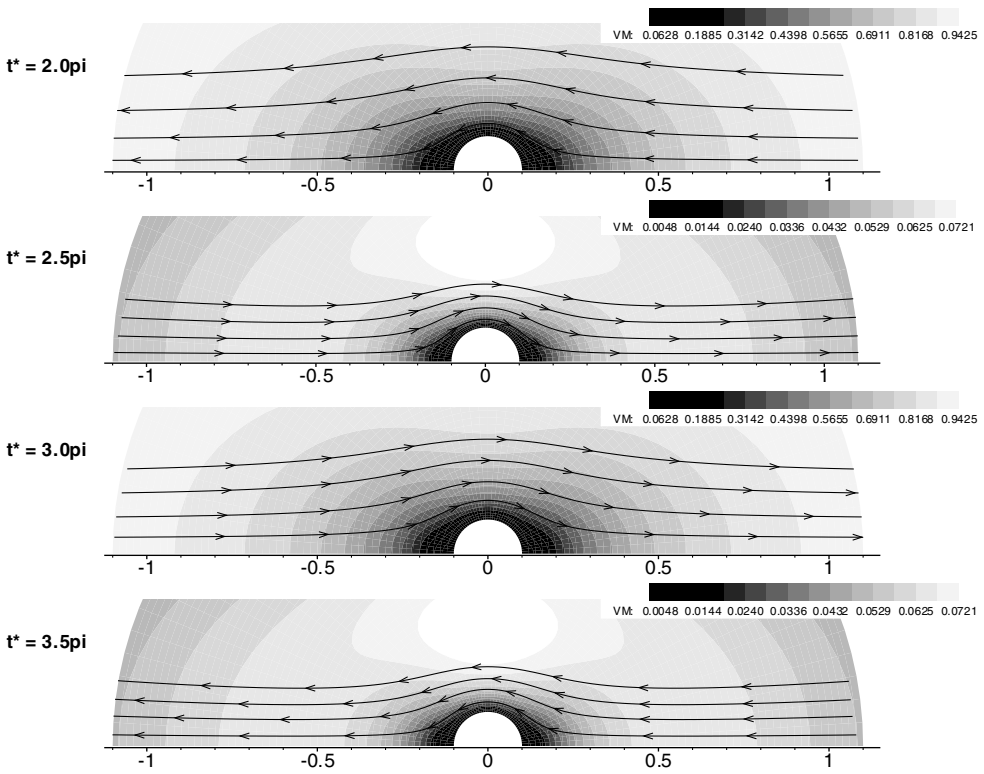

Fig. 4. Instantaneous flow field near the oscillating microdroplet.

may be related to the relaxation time of microdroplet. In the next half cycle of oscillation, similar flow patterns corresponding to 2π and 2.5π are reproduced at 3π and 3.5π, respectively, except that the flow direction has reversed.

5.3. Concentration field

The concentration field also exhibits the periodic characteristics of the oscillating microdroplet. Based on the numerical solution of Eq. (16) for various experimental parameters, such as the oscillation frequency, the maximum velocity, and the initial diameter of microdroplet, the instantaneous concentration distribution grayscale contours at various dimensionless instants, i.e., 2π, 2.5π, 3π and 3.5π, in a cycle are illustrated in Figs. 5–8, which correspond to the experimental parameters listed in Table 1. The concentration fields show clear wakes behind the microdroplet i.e., the concentration gradients in the forward part of the microdroplet are greater than those on the downstream side, because of the reduction of mass transfer on the upstream side of the microdroplet where the flow is in the opposite direction of the mass transfer, and the enhancement of mass transfer on the downstream side of microdroplet where the flow is in the same direction as the mass transfer. The concentration wakes in the first half cycle of oscillation are similar to those in the last cycle of oscillation except that the directions of the tails of concentration wakes are reversed.

We note that at the lower oscillation frequencies, which correspond to Figs. 5 and 6, the concentration wakes are much longer than the wakes shown in Figs. 7 and 8 for the higher frequency conditions. This phenomenon of the long wake also occurs in the case of mass transfer from a droplet moving at constant velocity. For an oscillating droplet the concentration distribution is limited to a region that decreases as the frequency increases because there is insufficient time for molecular diffusion to dominate the mass transport process. The concentration distribution within the mass transfer region is periodic to a certain extent as we show below.

5.4. Periodicity of the mass transfer

The periodic mass transfer characteristics calculated for the oscillating microdroplets are presented in Figs. 9–12. These figures show how the Sherwood number changes with dimensionless time for three different amplitudes of the oscillation. The amplitudes corresponding to the EDB experimental conditions are shown as solid lines, and the time-average Sherwood numbers obtained in the EDB experiments are also shown in each figure. At lower frequencies the instantaneous Sherwood

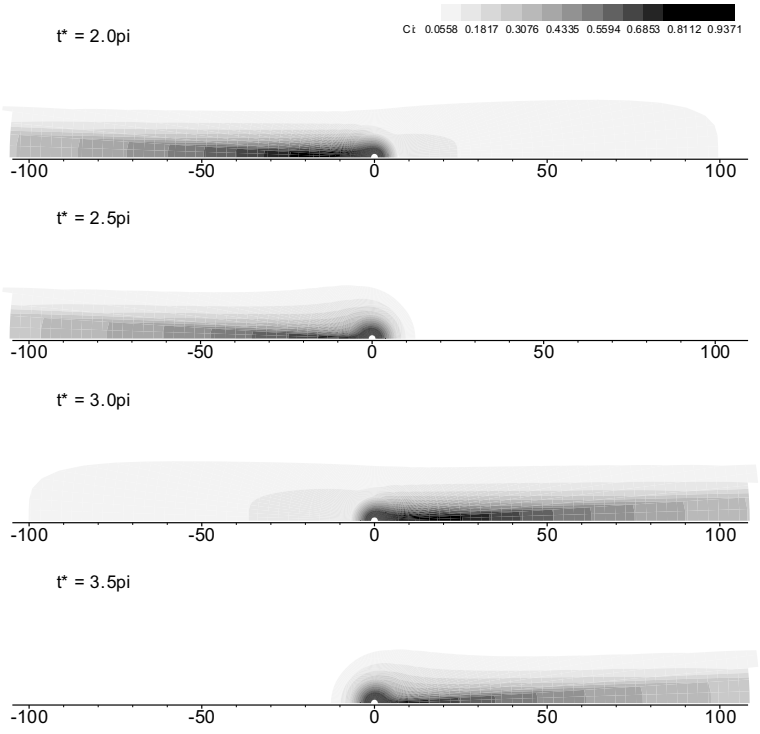

Fig. 5. Instantaneous concentration field for Case 1 of the experiments.

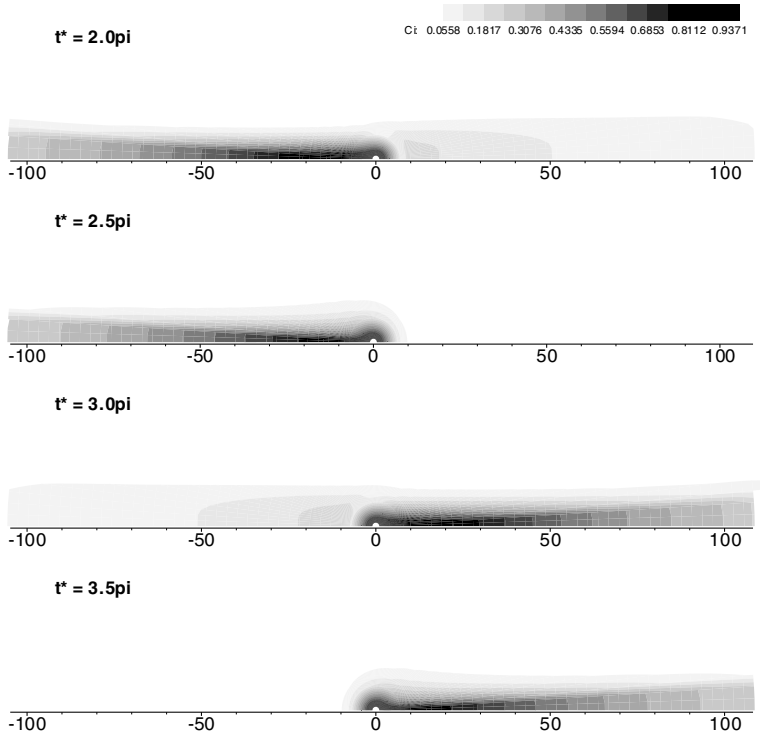

Fig. 6. Instantaneous concentration field for Case 2 of the experiments.

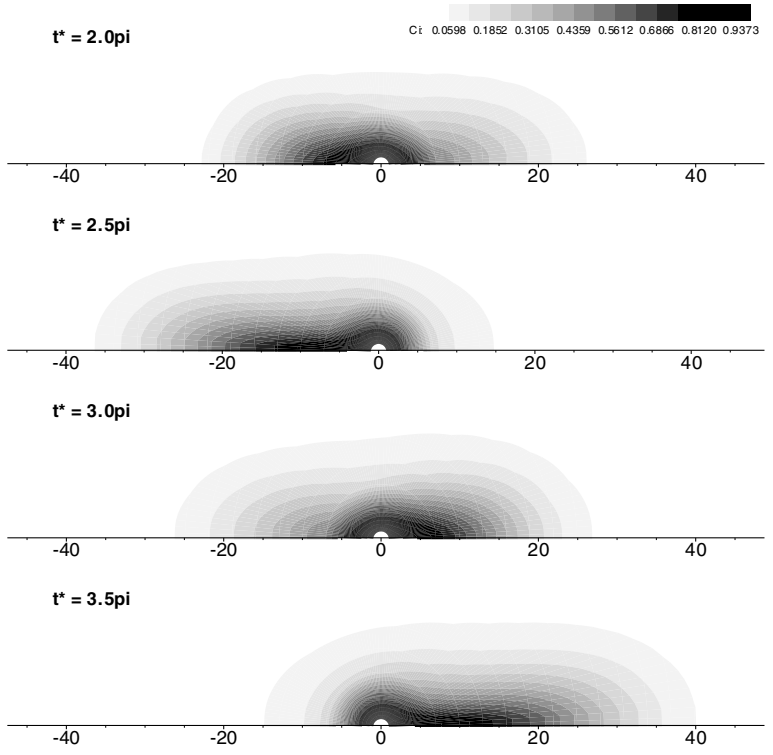

Fig. 7. Instantaneous concentration field for Case 3 of the experiments.

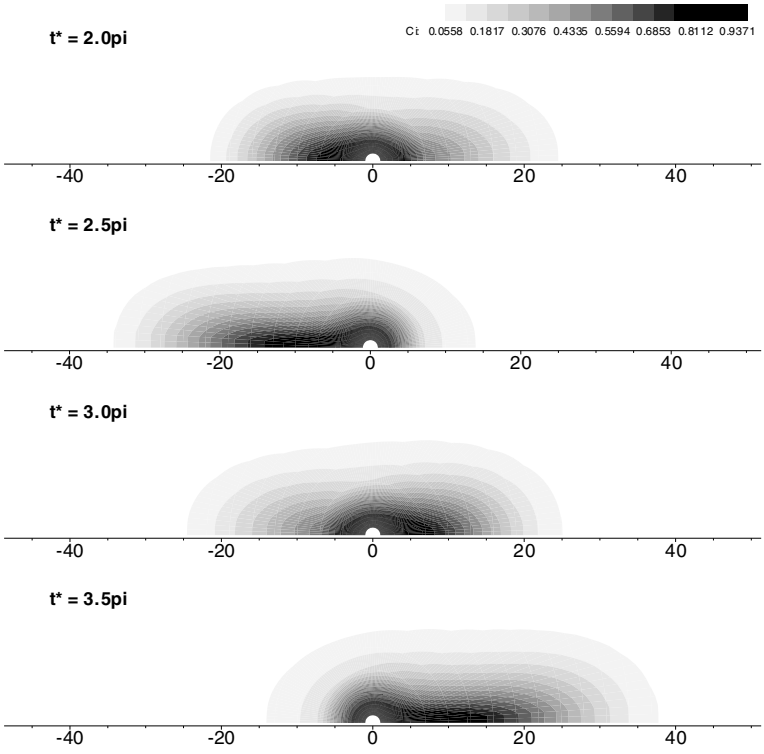

Fig. 8. Instantaneous concentration field for Case 4 of the experiments.

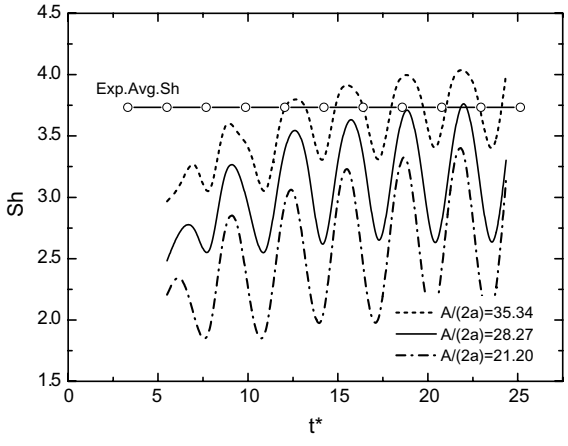

Fig. 9. Predicted Sh–t^* curves for various oscillatory amplitudes in 25 Hz.

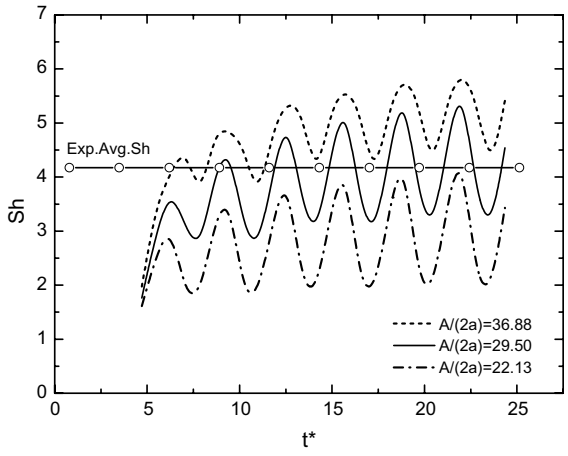

Fig. 10. Predicted Sh–t^* curves for various oscillatory amplitudes in 45.9 Hz.

numbers increase as the amplitude increases, but at higher frequencies Sh is essentially independent of the amplitude.

The periodic character of the mass transfer results from the periodic flow induced by the oscillating microdroplet. As seen in Figs. 9–12, Sh reaches a recurring periodic pattern after a few cycles. The trend of the average Sh shows a gradual change with time in the first few cycles. Initially, the microdroplet is stationary, so $Sh = 2$. As the oscillation of microdroplet proceeds, the convective flow enhances the mass transfer, so the average Sh increases with time. After a few cycles, the stable concentration distribution is formed, and the average Sh remains constant. The dimensionless period of the time-dependent Sherwood number is about π,

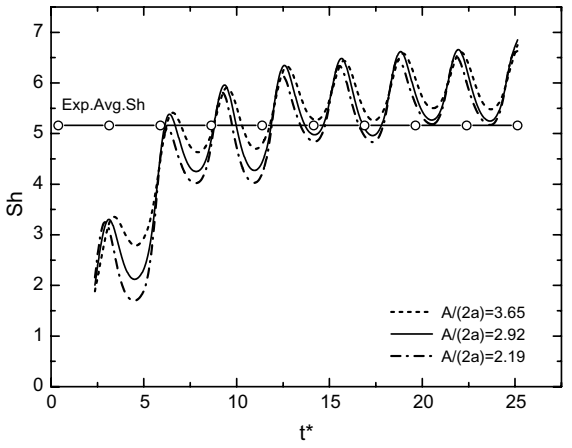

Fig. 11. Predicted *Sh–t** curves for various oscillatory amplitudes in 152.2 Hz.

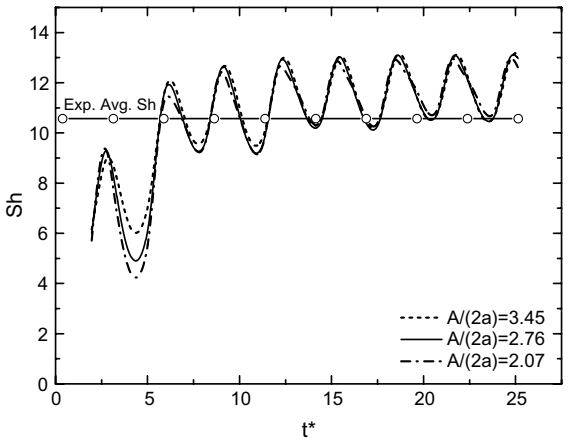

Fig. 12. Predicted *Sh–t** curves for various oscillatory amplitudes in 198.7 Hz.

which is one-half the dimensionless oscillatory period. This indicates that there is a symmetry associated with the mass transfer during an oscillation. During the first half of an oscillation cycle the mass transfer rate is the same as in the second half of the cycle. Consequently, the period associated with mass transfer is one-half the oscillation period.

6. Conclusions

The rate of mass transfer from an oscillating microdroplet can be significantly greater than the rate associated with a stationary droplet or a droplet in steady motion. The convective diffusion analysis provided here yields results in agreement with microdroplet evaporation experiments performed by Zhu et al. [9] with an electrodynamic levitator. Theory and experiment show that the mass transfer rate, expressed in terms of the Sherwood number, increases as the oscillation frequency increases and not merely with an increase in the streaming velocity. In addition, the analysis shows that the periodic characteristics of the mass transfer result from the periodic motion of the microdroplet, and the product of the Peclet and Strouhal number is indicative of the enhanced mass transfer rate.

Acknowledgments

The authors are grateful to National 863 High-Tech Project Foundation of China for grants 2002AA7020 and to the NSF for grant CTS-9982413 that supported the research.

References

[1] A. Prosperetti, Free oscillations of drops and bubbles: the initial-value problem, J. Fluid Mech. 100 (1980) 333–347.
[2] L.D. Landau, E.M. Lifshitz, Fluid Mechanics, second ed., Pergamon Press, Oxford, 1987.
[3] Z.D. Chen, X.D. Chen, J.J.J. Chen, Effect of an oscillating interface on heat transfer, Chem. Eng. Sci. 52 (1997) 3265–3275.
[4] Y.S. Mayya, Charging-induced drift and diffusion of aerosol particles in oscillating electric fields, J. Aerosol. Sci. 25 (1994) 277–288.
[5] R.I. Sujith, G.A. Waldherr, J.I. Jagoda, B.T. Zinn, Experimental investigation of the evaporation of droplets in axial acoustic fields, J. Propulsion Power 16 (2000) 278–285.
[6] Y. Tian, R.E. Apfel, A novel multiple drop levitator for the study of drop arrays, J. Aerosol. Sci. 27 (1996) 721–737.
[7] F. Mashayek, N. Ashgriz, Non-linear oscillations of droplets with internal circulation, Phys. Fluids 10 (1998) 1071–1082.
[8] F. Mashayek, Dynamics of evaporating drops, parts I: formulation and evaporation model, Int. J. Heat Mass Transfer 44 (2001) 1517–1526.
[9] J.H. Zhu, F. Zheng, M.L. Laucks, E.J. Davis, Mass transfer from an oscillating microsphere, J. Colloid Interface Sci. 249 (2002) 351–358.
[10] E.J. Davis, Microchemical engineering: the physics and chemistry of the microparticleAdvances in Chemical Engineering, vol. 18, Academic Press, London, 1992.
[11] A.M. Al Taweel, J. Landau, Mass transfer between solid spheres and oscillating fluids—a critical review, Can. J. Chem. Eng. 34 (1976) 532–539.
[12] E.J. Davis, G. Schweiger, The Airborne Microparticle, Springer-Verlag, Heidelberg, 2002.
[13] S.H. Zhang, E.J. Davis, Mass transfer from a single microdroplet to a gas flowing at low Reynolds number, Chem. Eng. Commun. 50 (1987) 51–67.
[14] V.G. Levich, Physicochemical hydrodynamics, Prentice Hall, New York, 1962.

[15] Z.H. Feng, J.H. Zhu, X.F. Yang, Numerical simulation of a single microparticle trajectory in an electrodynamic balance, Chin. J. Chem. Eng. 12 (2004) 444–447.
[16] P.E. Wagner, Aerosol growth by condensation, in: W.H. Marlow (Ed.), Chemical Physics of Microparticles, Topics in Current Physics, Volume 29: Aerosol Microphysics II, Springer-Verlag, Berlin, 1982.
[17] R. Chang, E.J. Davis, Interfacial conditions and evaporation rates of a liquid droplet, J. Colloid Interface Sci. 47 (1974) 65–76.
[18] D.C. Taflin, T.L. Ward, E.J. Davis, Electrified droplet fission and the Rayleigh limit, Langmuir 5 (1989) 376–384.
[19] J.H. Ferziger, M. Periç, Computational Methods for Fluid Dynamics, third ed., Springer-Verlag, Berlin, 2002.
[20] R.B. Bird, W.E. Stewart, E.N. Lightfoot, Transport Phenomena, second ed., John Wiley, New York, 2002.
[21] C.W. Hirt, A.A. Amsden, J.L. Cook, An arbitrary Lagrangian–Eulerian computing method for all flow speeds, J. Comput. Phys. 14 (1974) 227–253.
[22] R. Wei, A. Sekine, M. Shimura, Numerical analysis of 2D vortex-induced oscillations of a circular cylinder, Int. J. Num. Method. Fluids 21 (1995) 993–1005.
[23] F. Zheng, X. Qu, E.J. Davis, An octopole electrodynamic balance for three-dimensional microparticle control, Rev. Sci. Instrum. 72 (2001) 3380–3385.